






Article

Norfloxacin Loaded Lipid Polymer Hybrid Nanoparticles for Oral Administration: Fabrication, Characterization, In Silico Modelling and Toxicity Evaluation

Muhammad Asghar Khan ¹, Shahzeb Khan ^{1,2,*} , Mohsin Kazi ³ , Sultan M. Alshehri ³ , Muhammad Shahid ⁴, Shafi Ullah Khan ⁵, Zahid Hussain ^{6,7} , Muhammad Sohail ⁸ , Muhammad Shafique ⁹, Hajra Afeera Hamid ¹, Mahwish Kamran ¹, Abdelbary Elhissi ¹⁰, Muhammad Wasim ⁸ and Hnin Ei Thu ^{11,12}

- ¹ Department of Pharmacy, University of Malakand, Chakdara 18800, Pakistan; asghar247@yahoo.com (M.A.K.); afeera85@gmail.com (H.A.H.); arianmahwish@gmail.com (M.K.)
 - ² Discipline of Pharmaceutical Sciences, School of Health Sciences, University of KwaZulu Natal, Durban X54001, South Africa
 - ³ Department of Pharmaceutics, College of Pharmacy, King Saud University, Riyadh 11451, Saudi Arabia; mkazi@ksu.edu.sa (M.K.); salshehri1@ksu.edu.sa (S.M.A.)
 - ⁴ Department of Pharmacy, Sarhad University of Science and Information Technology, Peshawar 25000, Pakistan; shahidsalim_2002@hotmail.com
 - ⁵ Department of Pharmacy, Abasyn University Peshawar, Peshawar 25000, Pakistan; shafiullahpharmd@gmail.com
 - ⁶ Department of Pharmaceutics & Pharmaceutical Technology, College of Pharmacy, University of Sharjah, Sharjah 27272, United Arab Emirates; zhussain@sharjah.ac.ae
 - ⁷ Research Institute for Medical and Health Sciences (SIMHR), University of Sharjah, Sharjah 27272, United Arab Emirates
 - ⁸ Department of Pharmacy, COMSATS University Abbottabad Campus, Abbottabad 45550, Pakistan; Msmarwat@cuiatd.edu.pk (M.S.); wassypharmacist@gmail.com (M.W.)
 - ⁹ Department of Pharmaceutical Sciences, College of Pharmacy-Boys, Al-Dawadmi Campus, Shaqra University, Shaqra, Riyadh 11451, Saudi Arabia; shafiqueph@yahoo.com
 - ¹⁰ College of Pharmacy, QU Health and Office of VP for Research and Graduate Studies, Qatar University, Doha 2713, Qatar; aelhissi@qu.edu.qa
 - ¹¹ Research and Innovation Department, Lincoln University College, Petaling Jaya 47301, Malaysia; eithuu287@gmail.com
 - ¹² Innoscience Research Institute, Subang Jaya 47650, Malaysia
- * Correspondence: shahzebkh@uom.edu.pk; Tel.: +0092-345-9492-869



Citation: Khan, M.A.; Khan, S.; Kazi, M.; Alshehri, S.M.; Shahid, M.; Khan, S.U.; Hussain, Z.; Sohail, M.; Shafique, M.; Hamid, H.A.; et al. Norfloxacin Loaded Lipid Polymer Hybrid Nanoparticles for Oral Administration: Fabrication, Characterization, In Silico Modelling and Toxicity Evaluation.

Pharmaceutics **2021**, *13*, 1632. <https://doi.org/10.3390/pharmaceutics13101632>

Academic Editor: Ana Beloqui Garcia

Received: 17 August 2021

Accepted: 26 September 2021

Published: 6 October 2021

Publisher's Note: MDPI stays neutral with regard to jurisdictional claims in published maps and institutional affiliations.



Copyright: © 2021 by the authors. Licensee MDPI, Basel, Switzerland. This article is an open access article distributed under the terms and conditions of the Creative Commons Attribution (CC BY) license (<https://creativecommons.org/licenses/by/4.0/>).

Abstract: Norfloxacin (NOR), widely employed as an anti-bacterial drug, has poor oral bioavailability. Nano based drug delivery systems are widely used to overcome the existing oral bioavailability challenges. Lipid-Polymer Hybrid Nanoparticles (LPHNs) exhibit the distinctive advantages of both polymeric and liposomes nanoparticles, while excluding some of their disadvantages. In the current study, NOR loaded LPHNs were prepared, and were solid amorphous in nature, followed by in vitro and in vivo evaluation. The optimized process conditions resulted in LPHNs with the acceptable particle size 121.27 nm, Polydispersity Index (PDI) of 0.214 and zeta potential of -32 mv. The addition of a helper lipid, oleic acid, and polymers, ethyl cellulose, substantially increased the encapsulation efficiency (EE%) (65% to 97%). In vitro study showed a sustained drug release profile (75% within 12 h) for NOR LPHNs. The optimized NOR LPHNs showed a significant increase ($p < 0.05$) in bioavailability compared to the commercial product. From the acute toxicity study, the LD50 value was found to be greater than 1600 mg/kg. The molecular modelling studies substantiated the experimental results with the best combination of polymers and surfactants that produced highly stable LPHNs. Therefore, LPHNs proved to be a promising system for the delivery of NOR, as well as for other antibiotics and hydrophobic drugs.

Keywords: lipid polymer hybrid nanoparticles; norfloxacin; acute toxicity; oral bioavailability; in silico modelling

1. Introduction

In earlier centuries, infectious diseases triggered by numerous bacterial species were the primary cause of death [1]. Currently, mortality and morbidity rates of many infectious diseases have sharply declined with advancements in research in the arena of antibiotics [2]. Among the developed classes of antibiotics, Fluoroquinolones (FQs) have been reported as modern non-steroidal antibiotics/antibacterial [3]. Norfloxacin (NOR; Figure 1), a member of the FQs family, is a drug of choice for the diseases caused by *Escherichia coli*, *Vibrio cholerae*, *Shigella* and *Campylobacter* [4]. It is prescribed globally for the treatment of gonorrhoea, eye infections and urinary tract infections [5,6]. It works vigorously on dormant and dividing bacteria by inhibiting the bacterial enzyme DNA Gyrase. Its oral bioavailability is only 35–45% and half-life is 7 h [7]. Limited oral bioavailability represents its hydrophobic nature. This hydrophobic nature exacerbates its global image and thus drives pharmaceutical scientists to place it in Class-IV of the Biopharmaceutical Classification System (BCS-IV), representing low solubility and low permeability [8,9]. Various approaches, such as Solid Dispersion and Cyclodextrin inclusion complexes, have been used to improve the solubility and bioavailability of Norfloxacin [10,11]. There have been reports of some issues associated with the above approaches, which include scale up and physical stability [12,13].

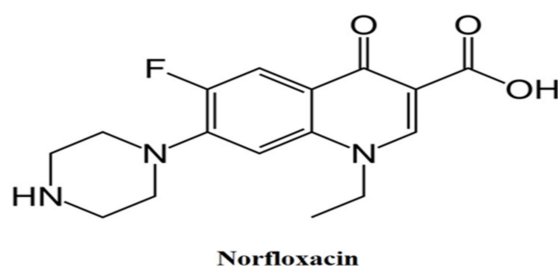


Figure 1. Chemical structure of norfloxacin.

Nanotechnology has become the most attractive platform for pharmaceuticals, with the potential to impact the delivery of a plethora of therapeutics including RNAs, small molecule therapeutic genes, diagnostic imaging agents and peptides [14]. The application of a drug delivery system demonstrates advantages in the modulation of a range of imperative attributes of drug compounds, including pharmacokinetics and pharmacodynamics properties, cellular targeting, molecular targeting and tissue targeting; targeted and non-targeted drug delivery to their relevant site [15,16].

Polymeric nanoparticles (NPs) and liposomes are the most well characterized among these nano-carrier types. Lipid polymer hybrid nanoparticles (LPHNs) have been developed as a hybrid nano-based delivery system, which has the structural integrity of the polymeric particles and the biomimetic properties of the liposome, and displays unique advantages of both nanoparticles while excluding some of their limitations [1,17]. The use of the distinct features of polymeric and liposome NPs has resulted in initial clinical triumph, but limitations must be controlled [18]. The hybrid system can be a strong delivery system platform with well tolerated serum stability, high encapsulation efficiency, well defined release kinetics and well triggered tissue, cellular, and molecular targeting properties. To the best of our knowledge, there has not yet been a study about NOR loaded LPHNs coupled with molecular modelling studies. Therefore, this study aimed to develop stable NOR-LPHNs for amplifying its water solubility and oral bioavailability. Eudragit Rs100 were used as a polymer, SA were used as solid lipids, while oleic acid and ethyl cellulose were used as helper lipids and polymers, respectively to enhance drug encapsulation. Owing to high permeability, independent pH swelling, stability and suitability for matrix forming structure attributes, Eudragit was chosen as the principal polymer [19]. Additionally, stearic acid was chosen because it is biodegradable, biocompatible and remains in a solid state at body temperature. Furthermore, it has been previously reported to have high

entrapment potential for NOR [20]. The molecular simulation study was also designed to identify the binding affinity of NOR with individuals and combinations of polymers, surfactant and helper lipids, and polymer molecules. The simulation study uncovered and underpinned molecular-level understanding of the configuration of NOR within a blend of polymers, surfactants and lipids. This study also endorsed the experimental findings about encapsulation efficiency of NOR within the hybrid system, and its impact on drug release kinetics. The NOR loaded LPHNs produced here were subjected to solid-state characterization and comparative in vivo and toxicity evaluation.

2. Materials and Methods

2.1. Material

NOR (Batch No. 20151218) was procured as a gift from Polyfine Pharma, Peshawar, Pakistan. Stearic acid (SA) (Batch No. D-7664-4400), Eudragit Rs100 (Batch No. D-6958-4406), ethyl cellulose (Batch No. D-4154-4405), sodium lauryl sulphate (Batch No. D-7592-1405) and oleic acid (Batch No. D-5635-4400) were purchased from Musa-G Chemicals, Peshawar, Pakistan. Other solvents and materials used in this study were of analytical grade.

2.2. Methods

2.2.1. Preparation of Unloaded LPHNs

LPHNs were produced via a combinative approach, using magnetic stirring and sonication (probe) [21]. The process parameters for the unloaded formulations are given in Table 1. For fabrication of unloaded LPHNs, SA was melted by heating up to 80 °C. Solution of Eudragit Rs100 and sodium lauryl sulphate (surfactant) was prepared in 80% ethanol and heated up to the same temperature (80 °C), followed by mixing with the melted lipid phase. To remove the organic solvent, the resultant mixture was stirred, followed by volume adjustment with water. Furthermore, the mixture was subjected to high intensity sonication (SONICS, NILOP195; Newtown, CT, USA) (30% amplitude) followed by cooling to produce the desired LPHNs dispersion.

Table 1. Blank LPHNs formulations.

Formulation Code	Stearic Acid (gm)	Eudragit (gm)	Sonication (Hz)	SLS	Sonication Time (min)	Stirring Time (min)
BF-1	0.5	1.0	30%	0.2	2	20
BF-2	0.5	1.0	30%	0.3	2	20
BF-3	0.5	1.0	30%	0.5	5	20
BF-4	0.5	1.0	30%	0.6	8	20
BF-5	0.5	1.0	30%	0.8	8	40
BF-6	0.5	1.0	30%	1.0	8	60

2.2.2. Preparation of Loaded NOR LPHNs

For fabrication of drug loaded LPHNs, NOR (20 mg) was added to the organic solution of polymer and surfactant. The process parameters for the NOR loaded LPHNs are given in Table 2. For co-encapsulation, oleic acid and ethyl cellulose were added to the organic solution of drug, polymer and surfactant followed by mixing with SA. Procedure followed thereafter was the same as mentioned for fabrication of unloaded LPHNs.

Table 2. Optimization of helper polymer and lipids for hybrid nanoparticles.

Formulation Code	Oleic Acid (mL)	Ethyl Cellulose (gm)
NOR-1	0	0
NOR-2	0.1	0
NOR-3	0.2	0
NOR-4	0.2	0.3
NOR-5	0.2	0.5

2.2.3. Lyophilization

Lyophilization/freeze drying is used to enhance the physical and chemical stability of LPHNs. Essentially, Lyophilization is employed for conversion of the nano-suspension to dry powder (solid dosage form), as well as to attain stability for prolonged period of time.

Before drying, glucose solution (10%) was added as cryoprotectant to avoid aggregation of LPHNs. LPHNs were kept overnight at $-20\text{ }^{\circ}\text{C}$ and then shifted to the freeze dryer to be lyophilized at $-75\text{ }^{\circ}\text{C}$ for 48 h at an increasing rate of $5\text{ }^{\circ}\text{C/h}$ [22].

2.2.4. Entrapment Efficiency and Drug Loading Capacity

Five different nano-formulations of NOR-LPHNs were subjected to the calculation of drug entrapment efficiency and drug loading capacity, using the following formulae.

$$\text{EE\%} = \frac{(\text{Total amount of drug added} - \text{Unloaded Drug}) \times 100}{(\text{Total amount of drug added})} \quad (1)$$

$$\text{DLC\%} = \frac{(\text{Total amount of drug in LPHNs}) \times 100}{(\text{Amount of Drug Added} + \text{Amount of Excipients})} \quad (2)$$

2.2.5. Characterization

Dynamic Light Scattering

Particle analysis was carried out using a zeta-sizer (Microtrac Nanotrac wave II (USA)). Z-average particle size, PDI, and zeta potential were analyzed. LPHNs formulations were diluted with deionized water in order to get proper scattering intensity, measured at a 90° scattering angle and $25\text{ }^{\circ}\text{C}$.

Drug-Excipients Interaction

Fourier transform infrared spectroscopy (IR Prestige 21, Shimadzu, Kyoto, Japan) was used to study drug-excipients interaction. Spectra of unprocessed NOR and processed NOR (NOR-5) were scanned over a frequency range of 4000 to 450 cm^{-1} . For compatibility of drug with formulation components, the peaks and patterns shaped by the unprocessed NOR were compared with processed NOR (NOR-5).

Scanning Electron Microscopy (SEM)

Scanning electron microscopy was used to study the morphological characteristics and texture of LPHNs by JSM5910 (JEOL, Tokyo, Japan). SEM micrographs were recorded at accelerating voltage of 15 kV .

Powder X-ray Diffraction (P-XRD)

Powder X-ray diffraction analysis was performed to verify new solid state formation [23]. P-XRD analysis was conducted for unprocessed NOR and processed NOR (NOR-5) using X-ray Diffractometer JDX-3532 (JEOL, Tokyo, Japan). $\text{Cu K}\alpha$ radiation in a scanning range of $2\theta = 5^{\circ}$ – 50° was used with tube current 30 mA , operated voltage of 40 kV , step time of 1.0 sec , step size of 0.05° , divergence slit of 1 degree , scattering slit of 1.0 degree , and receiving slit of 0.2 mm for measurement.

Differential Scanning Calorimetry (DSC)

Differential scanning calorimetry (DSC) is a thermo analytical method used to investigate melting and recrystallization behavior of samples. Accurately weighted unprocessed NOR, stearic acid, their physical mixture and processed NOR (NOR-5) were analyzed by DSC (Diamond Series DSC Equipment, Perkin Elmer, Waltham, MA, USA). Analyses were carried out in crimped aluminum pans at the heating rate of $10\text{ }^{\circ}\text{C/min}$ from 40 – $400\text{ }^{\circ}\text{C}$.

Stability Study

It is imperative to monitor the physical and chemical stability of the produced nanoparticles at elevated temperatures [24]. The stability study was conducted at various temperatures, to examine the physical stability of NOR-LPHNs. The freshly fabricated sample was divided into two parts. Each part was put in two plain sealed glass vials and stored at different temperatures (4 ± 1 °C and 25 ± 3 °C) for 3 months. Samples were taken on the 1st, 15th, 30th, 60th, and 90th day of storage and subjected to particle size and PDI measurements. Data were analyzed statistically by two tailed t-test. Probability < 0.05 was considered significant.

In Vitro Release of NOR from LPHNs

An in vitro drug release study was conducted using the dialysis bag method [25]. Dialysis bags were soaked in deionized water for 12 h before use. NOR-LPHNs dispersion (1 mL) from each formulation was poured into the dialysis bag and placed in 250 mL phosphate buffer solution (pH 7.4) at 50 rpm. After a defined time interval (1–12 h), samples were taken and equal volume of phosphate buffer solution was replaced to make the final volume. Samples were analyzed using a UV spectrophotometer (λ max 278 nm) against blank phosphate buffer solution (pH 7.4) [26]. Data obtained from the in vitro drug release study were fitted into different kinetic models to find out both the drug release rate and mechanism followed [27].

Pharmacokinetic Evaluation

For pharmacokinetic evaluation, Sprague-Dawley rats weighing 150–200 gm were used. This study was conducted as per guidelines approved by the ethical committee of the University of Malakand (Chakdara, Pakistan. Notification Ref: Pharma/ECC/HA-112-4-15). The rats were fasted for 24 h prior to the experiment with free access to water. The animals were randomly divided into four groups with each group consisting of six (6) animals ($n = 6$). The animals were orally administered with pure norfloxacin, norfloxacin nanoparticles, as well as marketed drugs at a dose equivalent to 20 mg/kg. The blood samples were collected from the retro-orbital plexus at specific intervals of 0.08, 0.25, 0.50, 1, 2, 4, 6, 8, 12, and 24 h. To compensate the loss of blood, equal volume of normal saline was injected to animals. The blood samples were centrifuged at 7000 rpm at 4 °C for 20 min to separate plasma. Separated plasma samples were analyzed via the high performance liquid chromatography method as previously reported [28].

Acute Toxicity

An acute toxicity test was performed according to the chemical testing guidelines of the Organization for Economic Co-operation for Development (OECD) [29]. Animals were divided into numerous groups, each group having six (6) mice. Nano-formulation was orally administered at doses of 50, 100, 200, 400, 800 and 1600 mg/kg. Morbidity was observed continuously for the initial two (2) h and mortality was observed after 24 h, post-dose administration. The animals were observed for gross behavioral changes. The 50% mortality among the animals was calculated using probit analysis.

Molecular Modelling

The structure of NOR, ethyl cellulose (EC), eudragits, oleic acid (OA), sodium lauryl sulphate (SLS) and stearic acid were downloaded from PubChem. Energy minimization of all generated structures were carried out using YASARA-Structure software [30]. The structures of all ethyl cellulose, eudragits, oleic acid, sodium lauryl sulfate (SLS) and stearic acid polymers were considered as alternative receptors (host) and ligands (guest) to obtain the stable complex of co-polymeric structure, while Norfloxacin was used only as a ligand (guest) structure for the molecular docking simulations. AutoDock Vina was used for molecular docking calculation in PyRx [31], in which the grid box was set to cover the entire polymer to ensure that all possible interactions with the drug were searched [32].

The best docked complex between co-polymer and drug was then subjected to molecular dynamics (MD) to divulge its stability in time and under the influence of explicit solvent molecules. MD simulations were carried out in YASARA-Structure program using the YASARA force field with knowledge-based components [30]. Chimera and Discovery Studio Visualizer were used for the visualization and graphical representations of all co-polymer and drug complex [33].

Statistical Analysis

The produced data was statistically analysed by taking mean and \pm standard deviation of all the values. One way analysis of variance (ANOVA) and *t*-tests were used to calculate the *p* values in all calculations, where a *p*-value < 0.05 was considered in the significant range for comparison. For calculations of PK (pharmacokinetics) parameters, WinNonLin (v 4.0; Pharsight Corporation Inc., Mountain View, CA, USA) was used.

3. Results

3.1. Preparation of LPHNs

The process and experimental conditions were evaluated for fabrication of LPHNs using an integrated technique of probe sonication and magnetic stirring. Unloaded LPHNs were prepared on the basis of three variables i.e., surfactant concentration, magnetic stirring time and sonication time.

The best unloaded formulation (BF-6) showed an average particle size of 115.25 nm (Table 3), while the optimized drug loaded formulation (NOR-5) showed an average particle size of 121.27 nm, PDI (0.214) and zeta potential (-32 mV). There was, however, an observed slight increase in PDI, zeta potential and particle size of the optimised NOR loaded LPHNs. Prior to adding the helping polymer and lipid, the values of PDI, particle size and zetapotential were 0.20, 115.5 nm and -28.0 mV

Table 3. Process and experimental conditions for preparation of blanks nanoparticles.

Formulation Code	Stearic Acid (gm)	Eudragit (gm)	Sonication (Hz)	SLS	Sonication Time (min)	Stirring Time (min)	Particle Size (nm) \pm SD
BF-1	0.5	1.0	30%	0.2	2	20	605.41 \pm 5.0
BF-2	0.5	1.0	30%	0.3	2	20	445.34 \pm 4.5
BF-3	0.5	1.0	30%	0.5	5	20	310.76 \pm 5.0
BF-4	0.5	1.0	30%	0.6	8	20	140.82 \pm 4.0
BF-5	0.5	1.0	30%	0.8	8	40	129.53 \pm 3.0
BF-6	0.5	1.0	30%	1.0	8	60	115.25 \pm 2.5

3.2. Entrapment Efficiency (EE %) and Drug Loading Capacity (DLC %)

For optimization, in terms of EE % and DLC % varied concentration of ethyl cellulose (co-polymer) and oleic acid (co-lipid) were employed. On the basis of varied concentrations of ethyl cellulose and oleic acid five (5) formulations were designed i.e., NOR-1 to NOR-5 (Table 4).

Table 4. Impact of helper lipid and polymer on EE % and DLC %.

Formulation Code	Oleic Acid (mL)	Ethyl Cellulose (gm)	EE (%)	DLC (%)
NOR-1	0	0	65 \pm 2.08	0.258
NOR-2	0.1	0	71 \pm 2.51	0.272
NOR-3	0.2	0	79 \pm 1.52	0.291
NOR-4	0.2	0.3	89 \pm 0.1	0.295
NOR-5	0.2	0.5	97 \pm 1.52	0.302

Table 4 showed that EE % and DLC % increased significantly with the addition of helper polymer and helper lipid (Figure 2). EE % and DLC % for the optimized nano-formulation (NOR-5) was 97% and 0.302%, respectively.

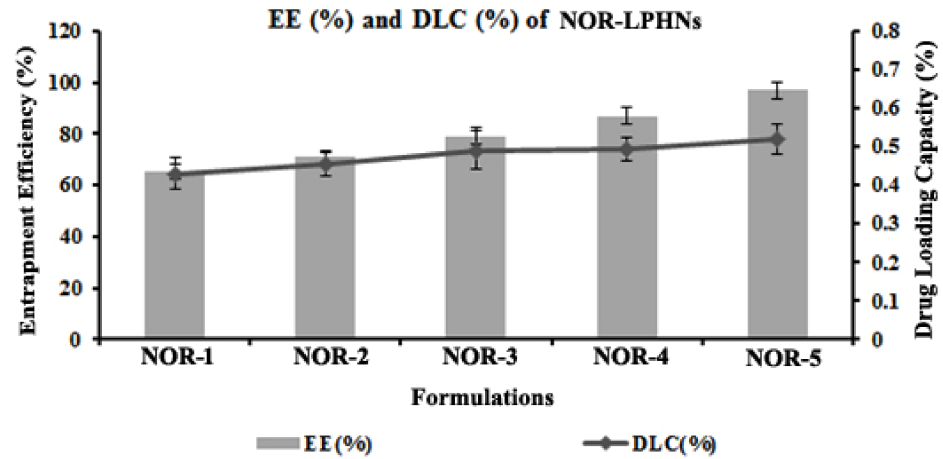


Figure 2. EE and DLC of the prepared formulations.

3.3. Drug Excipients Interaction

Norfloxacin showed major characteristic peaks at 2913.68 cm^{-1} due to =CH and aromatic –H stretching, and 2852.18 cm^{-1} due to CH_2 stretch, 1751.69 cm^{-1} due to –C=O stretching, 1619.33 and 1578.89 cm^{-1} due to quinolones N–H bending, 1383.07 cm^{-1} due to O–H bending. Neither spectra showed prominent changes in peak positions. Results revealed the absence of any chemical interaction between drug and excipients (Figure 3).

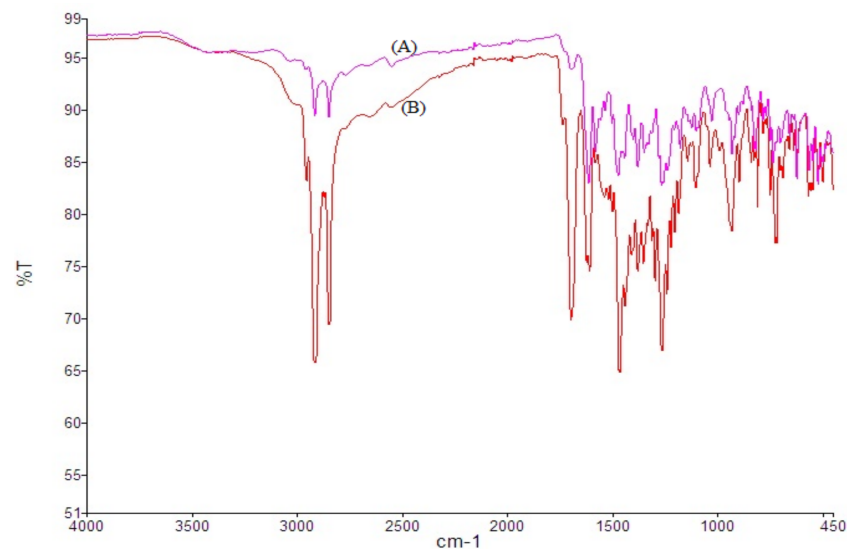


Figure 3. FT-IR spectra of unprocessed NOR (A) and processed NOR-5 (B).

3.4. Scanning Electron Microscopy (SEM)

Scanning electron microscopy was used to check the surface morphology and shape of the prepared NOR LPHNs formulation. SEM micrographs showed nanometric range spherical shaped white patches, which were uniformly distributed (Figure 4).

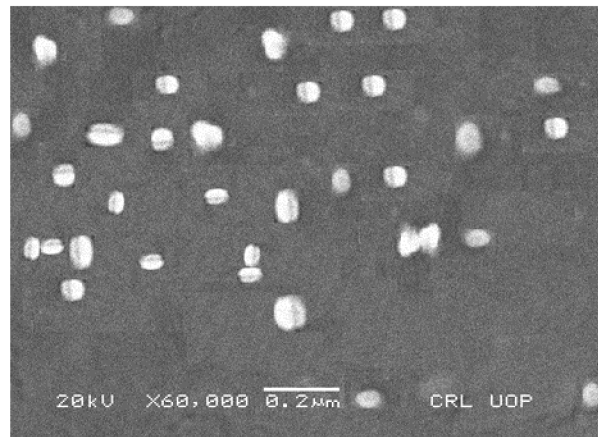


Figure 4. SEM micrograph of NOR-5 formulation.

An aggregate of the particles was not found. It is obvious that the process and experimental parameters were sufficiently controlled for engineering the hybrid nanoparticles with homogenous distribution.

3.5. X-ray Diffraction

Powder X-ray diffraction was performed to determine crystallinity of the fabricated nano-formulation. The unprocessed formulation showed sharp peaks indicating its crystalline nature, while for processed norfloxacin, some of these peaks were diffused indicating its conversion to semi crystalline form (Figure 5).

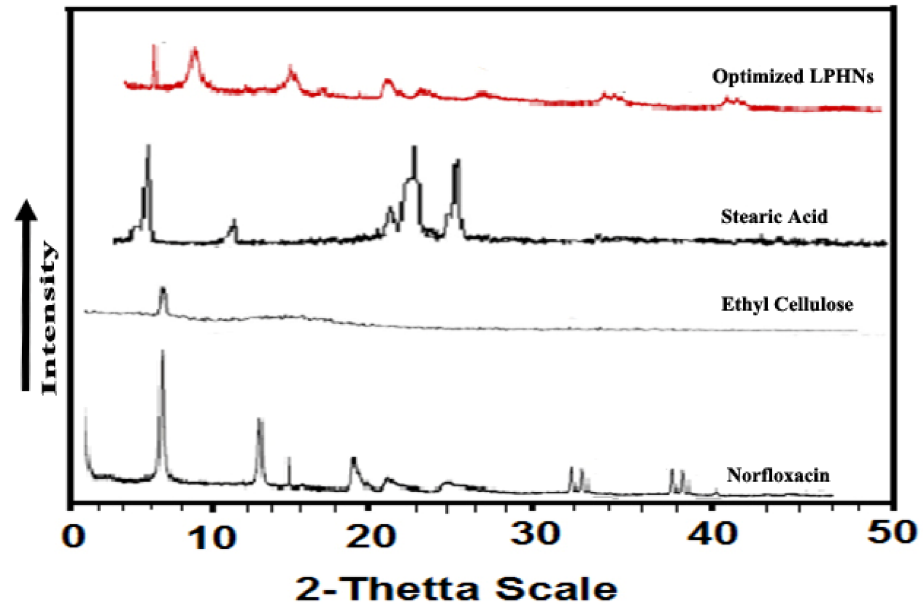


Figure 5. P-XRD of stearic acid, ethyl cellulose as well as processed (NOR-5) and unprocessed NOR.

3.6. Differential Scanning Calorimetry (DSC)

A DSC study was carried out to understand the melting points. The DSC study was performed for unprocessed norfloxacin, processed norfloxacin, ethyl cellulose and stearic acid (Figure 6).

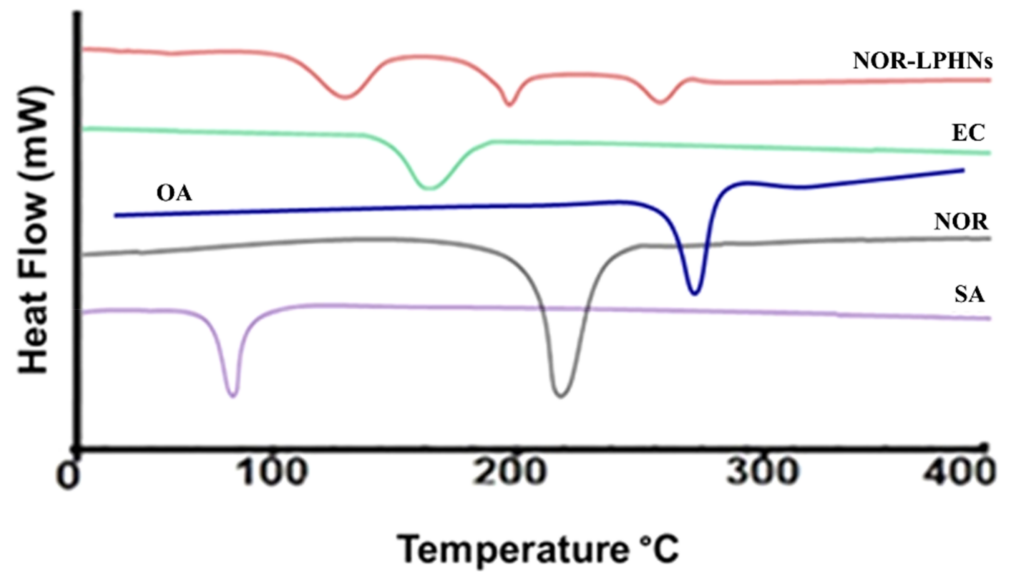


Figure 6. DSC thermogram of norfloxacin (NOR), ethyl cellulose (EC), stearic acid (SA), oleic acid (OA) and NOR-5-LPHNs.

Successful entrapment of NOR within the lipid polymer hybrid system was authenticated by the DSC studies.

3.7. Stability Study

A stability study was performed for the prepared NOR-LPHNs formulation at various temperatures (4 °C and 25 °C). Results showed that NOR nano-formulation was stable at both temperatures. No significant changes were observed in the particle size or PDI of the formulation (Figures 7 and 8).

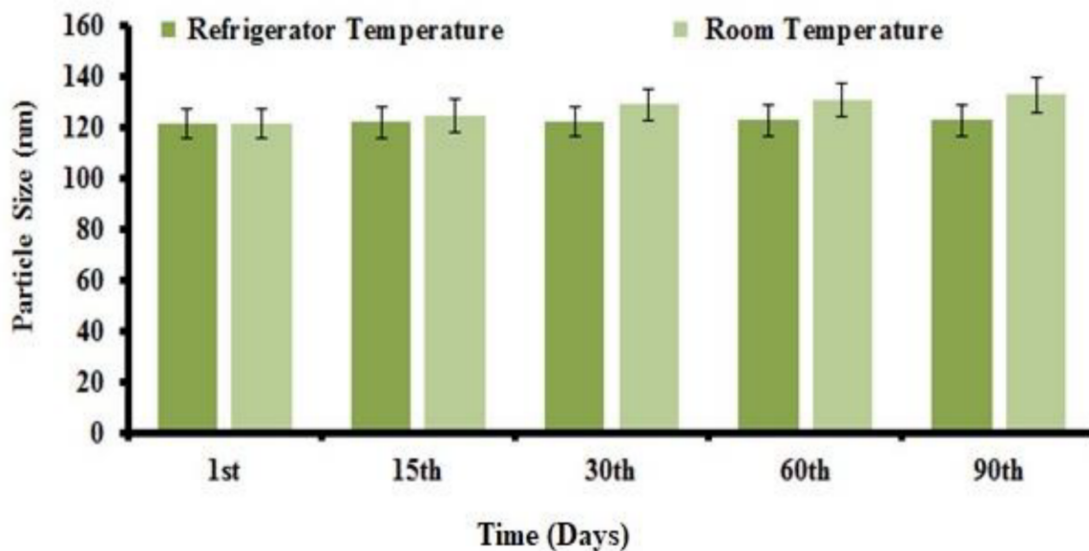


Figure 7. Particle size distribution of NOR-5 as a function of time. Refrigerated temp; (4 °C) and Room Temp; (25 °C).

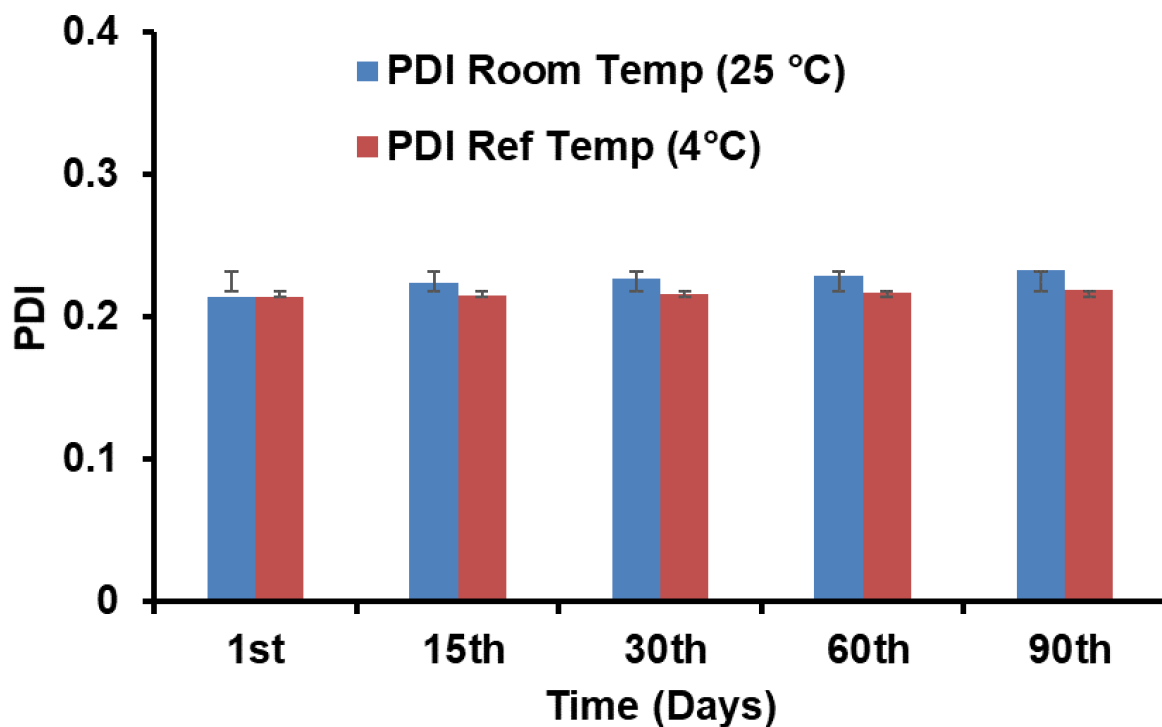


Figure 8. PDI of NOR-5 as a function of time. Ref; Refrigerated.

3.8. In Vitro Drug Release

In vitro release of drugs from LPHNs can be altered by appropriate selection of the lipid type, surfactant/co-surfactant concentration, as well as fabrication variables [34].

In vitro study revealed that NOR loaded LPHNs initially showed maximum (burst) release (Figure 9). The formulations including NOR1-NOR-3 showed that almost >90% of the total NOR was released over 12 h. Furthermore, the NOR-4 and NOR-5 formulations exhibited almost 80% and >75% release of the NOR from the hybrid system, respectively.

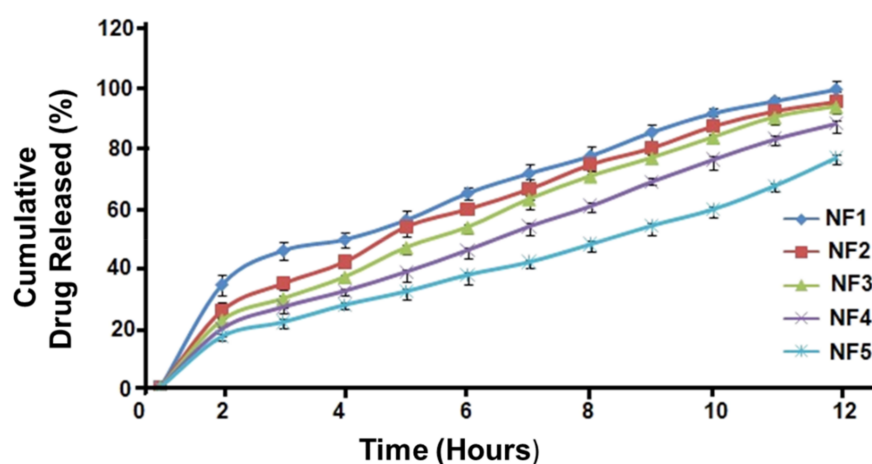


Figure 9. Drug release pattern for NOR nano formulations.

3.9. Kinetic Modeling

A kinetic modeling study was conducted for the produced nano-formulations to predict the rate and mechanism of drug release (Table 5). In the Korsmeyer–Peppas model, the value of n (the release exponent) exceeded 0.5 ($n > 0.5$). This confirmed non-Fickian diffusion kinetics (anomalous transport), i.e., drug release followed by both erosion/dissolution

of the lipid matrix as well as diffusion of the drug from LPHNs [35,36]. However, due to high value of the correlation coefficient (R^2) which ranges (0.935–0.981), Zero Order model was found the best fit for the drug release data.

Table 5. Kinetic models for various NOR formulations.

Formulation	Zero Order (R^2)	First Order (R^2)	Higuchi Model (R^2)	Korsmeyer-Peppas (n)	Korsmeyer-Peppas (R^2)
NOR-1	0.935	0.891	0.920	0.683664	0.941
NOR-2	0.946	0.975	0.934	0.747877	0.943
NOR-3	0.953	0.941	0.945	0.807612	0.945
NOR-4	0.977	0.953	0.969	0.878347	0.955
NOR-5	0.981	0.948	0.980	0.903442	0.967

3.10. In Vivo Study

Figure 10 is depicting the PK (Pharmacokinetics) parameters in terms of plasma concentration-time for NOR, optimized nanoparticles and optimized nano-formulation along with a marketed formulation of an equivalent dose of 20 mg/kg body weight. The various pharmacokinetic factors AUC, C_{max} , T_{max} and $t_{1/2}$ are represented in Table 6.

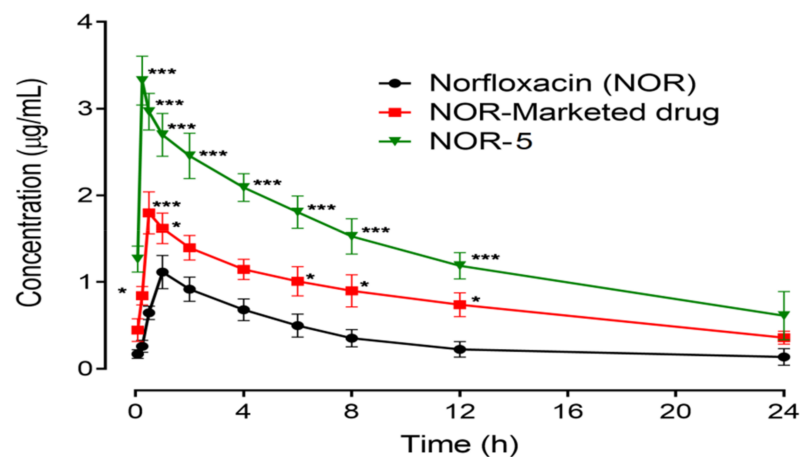


Figure 10. Pharmacokinetic profile of Norfloxacin (NOR), Norfloxacin nanoparticles (NOR-Nano) and Norfloxacin marketed drug (NOR-Marketed drug). Plot of plasma concentration ($\mu\text{g}/\text{mL}$) vs. time (h). Data presented as mean \pm SEM. * $p < 0.05$, *** $p < 0.001$ as compared to Norfloxacin treated rats at respective time-period. Two-way repeated measures ANOVA followed by *post hoc* Bonferroni's analysis.

Table 6. Pharmacokinetic parameters for Norfloxacin (NOR), its nanoparticles (NOR-Nano), nano-dosage form (NOR-Nano dosage form) and marketed drug (NOR-Marketed drug).

Sample	Pharmacokinetic Parameter			
	$T_{1/2}$ (h)	T_{max} (h)	C_{max} ($\mu\text{g}/\text{mL}$)	AUC _{0-t} ($\mu\text{g h}/\text{mL}$)
Norfloxacin	4.037 \pm 2.024	1.10 \pm 0.654	1.133 \pm 0.1856	8.600 \pm 2.511
NOR-Nano	26.07 \pm 3.273 ***	0.31 \pm 0.874 **	3.333 \pm 0.2963 ***	33.23 \pm 4.486 **
NOR-Marketed drug	8.64 \pm 1.497 *	0.54 \pm 1.021	1.833 \pm 0.2404	19.30 \pm 3.118 *

Values are expressed as mean \pm SD. One-way repeated measures ANOVA followed by Dunnett's *post hoc* test. * $p < 0.05$, ** $p < 0.01$, *** $p < 0.001$ as compared to pure NOR treated group, $n = 6$.

Pharmacokinetic profile of NOR at a dose of 20 mg/kg showed a higher concentration value of 1.13 $\mu\text{g}/\text{mL}$ at 1.0 h with an area under the concentration-time curve from time zero to 24 h observed as 8.6 $\mu\text{g h}/\text{mL}$ and an elimination half-life of 4.0 h. The comparative

marketed formulation of NOR showed a significant amplification in the area under the plasma drug concentration ($19.3 \mu\text{g h/mL}$, $p < 0.05$), and elimination half-life (8.6 h , $p < 0.05$), while no significant modification was identified in the maximum plasma NOR concentration ($1.8 \mu\text{g/mL}$) and the time to reach maximum drug concentration (0.54 h), in contrast to the pure drug. Optimized NOR nanoparticles revealed considerable changes in the pharmacokinetics of NOR and were noted as a noteworthy rise in the maximum peak plasma concentration ($3.33 \mu\text{g/mL}$, $p < 0.001$), AUC ($33.2 \mu\text{g h/mL}$, $p < 0.01$), and elimination half-life (26 h , $p < 0.01$), with a considerable reduction in the time of maximum concentration (0.31 h , $p < 0.01$), as compared to the pure NOR drug. In addition, the core of LPHNs has been reported to be super resistive to the external biological environment to keep the drug in stable form with subsequent high concentration in blood stream [37].

3.11. Acute Toxicity

During the initial two (2) h of morbidity assessment, behavioral changes were not observed for NOR nanoparticles. After 24 h of post-dose administration in the range of 50–400 mg/kg, no mortality was noted (Table 7), while a subsequent increase in the dose was associated with a slight increase in mortality. A mortality of 16.6% was noted with a dose of 800 mg/kg, while mortality increased up to 33.3% when the dose was increased to the experimental high-dose of 1600 mg/kg. From this acute toxicity profile of NOR nanoparticles, the LD_{50} value was considered to be higher than 1600 mg/kg.

Table 7. In vivo acute toxicity test of norfloxacin nanoparticles.

Dose (mg/kg)	No. of Dead Mice	Percent Lethality	LD_{50} (mg/kg)
50	0	00.00	
100	0	00.00	
200	0	00.00	
400	0	00.00	>1600
800	1	16.66	
1600	2	33.33	

3.12. Molecular Modelling

Molecular docking is an important modelling approach that gives an idea about the interactions between receptor (host) and ligand (guest). This in-silico method allows us to depict the ligand binding sites and conformations within a host. Mostly, the molecular docking simulation gives insight about the orientation of the drug in a binding site (termed as 'pose'), and also gives an estimation of the binding affinity of the identified pose in the form of a scoring value [32]. The AutoDock-VINA algorithm utilizes a 'machine-learning' method that merges the advantages of knowledge-based potentials and empirical scoring-functions to calculate the binding energy of a given ligand pose. The relative binding free energies between the NOR and different polymer molecules, as well as co-polymeric molecules, were calculated using Autodock Vina, as indicated in Table 8. The binding free energies between an ethyl cellulose, eudragits, oleic acid, sodium dodecyl sulfate (SLS), stearic acid (host) and NOR molecule (guest) will estimate the strength of the interactions between them. Tighter interactions between the drug molecules and polymer might lead to a stable drug-polymer complex, and may result in a more sustained drug release profile than when compared to looser interaction/binding [38,39]. It was also apparent from the binding free energies table that the mono-polymeric form has a lower binding affinity than the co-polymeric form. For example, mono-polymeric complexes including Stearic Acid-NOR, SLS-NOR, Eudragit-NOR and Oleic Acid-NOR (-2.4 kcal/mol) complexes were found to have the least binding affinity compare to Ethyl Cellulose-NOR (-3.4 kcal/mol). The bare co-polymeric complex between NORF-polymer was found to have lower binding affinity compared to their co-polymer complex with NOR. The complex with the best binding affinity and binding energy was the co-polymer complex of Stearic Acid-Eudragit-

SLS-OA-EC-NOR which was -5.9 kcal/mol, followed by Stearic Acid-Eudragit-SLS-NOR (-5.2 kcal/mol) as shown in Table 8.

Table 8. Binding energies calculations for different Co-polymeric systems of SLS, Eudragit, HPMC and NOR.

S. No	Co-Polymer Complex	Binding Energies (kcal/mol)
1	Stearic Acid-NOR	-2.4
2	SLS-NOR	-2.4
3	Eudragit-NOR	-2.3
4	Oleic Acid-NOR	-2.5
5	Ethyl Cellulose-NOR	-3.4
6	Stearic Acid-Eudragit-SLS-NOR	-5.2
7	Stearic Acid-Eudragit-SLS-OA-EC-NOR	-5.9

In order to comprehend the binding mode, interaction mechanism, and complex stability between the NOR and co-polymers complex, MD simulations were also performed. The stability of the simulated systems was assessed by measuring the differences in the root mean square deviation (RMSD) in relation to the minimized structures. MD simulation also revealed the stability of co-polymeric complexes with NOR. The binding orientation of NOR within the complex structure of Stearic Acid-Eudragit-SLS-OA-EC-NOR is shown in Figure 11.

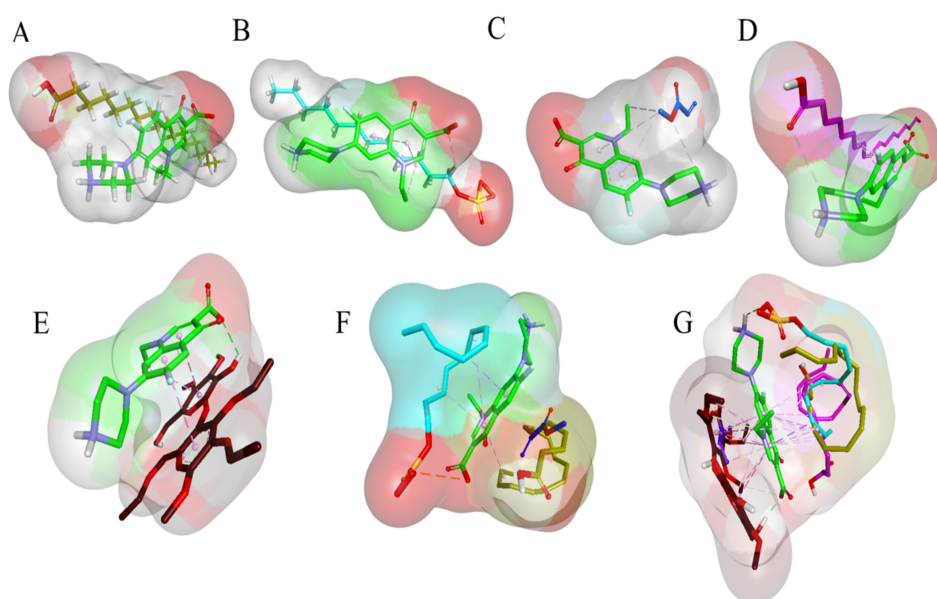


Figure 11. Structure of polymer and drug complex. (A). 3D surface and structure representation of Stearic Acid-NOR complex, (B). 3D surface and structure representation of SLS-NOR complex, (C). 3D surface and structure representation of Eudragit-NOR complex, (D). 3D surface and structure representation of Oleic Acid-NOR complex structure, (E). 3D surface and structure representation of Ethyl Cellulose-NOR complex structure, (F). 3D surface and structure representation of Stearic Acid-Eudragit-SLS-NOR complex, (G). 3D surface and structure representation of Stearic Acid-Eudragit-SLS-OA-EC-NOR complex structure.

Moreover, the interaction of lipids and co-polymers with drug molecules can also be rationalized. A favorable complex can be formed with lipids and helping polymers that can heighten the interaction with NOR.

4. Discussion

LPHNs were optimized via changing variable parameters. Variable parameters can result in efficient micro-mixing and high energy input that can lead to small particle size and narrow size distribution [40]. Strength in tiny droplets of lipid was provided by increasing the concentration of surfactant, resulting in the prevention of coalescence [40]. Particle size and zeta potential of the prepared nanoparticles were increased after drug loading and with the addition of excipients [41]. The process parameters, including stirring time, sonication time and SLS concentration, were found to be the key parameters to greatly influence particle size and PDI of the produced LPHNs. A substantial reduction in the particle size of the produced nanoparticles was observed with high stirring and sonication time, compared to a small period of time. Both of these factors result in a high level of micromixing and molecular diffusion, which is paramount for the production of small and stable nanoparticles [42–44]. The efficient micromixing of the two phases results in high levels of supersaturation and fast nucleation that minimizes the number of solute molecules available for aggregation and growth with the subsequent stable nanoparticles. Our optimization experiments clearly demonstrated a sharp decreasing pattern in the particle size with an increasing stirring and sonication time. Furthermore, the SLS concentration also demonstrated a significant impact on the reduction of the particle size of the produced nanoparticles. At high SLS concentrations, the surface tension is reduced, leading to enhanced particle partition [45]. The swift particle partition results in a significant decrease in particle size with a large surface area. Here, competition between the two kinetic and diffusion processes, including coverage of the newly formed surfaces and aggregation of the already existed particles, is commenced. With a high concentration of the surfactants, SLS rapidly covers the newly formed surfaces while hindering the aggregation of the particles. However, there is an optimum concentration level above which the concentration is not effective enough to stop the particle growth. It has also become evident from our experiment that the particle size sharply decreased with increasing concentration of SLS. On the basis of the optimized conditions, BF-6 was found to be the most suitable formulation for onward process. However, for the interaction between factors to impact the particle size of the LPHNs, a proper factorial design is required. An optimized LPHNs system demonstrated an adequate value of zeta potential, revealing electrostatic stability for the nanosuspension. The resultant zeta potential ± 30 and PDI < 0.5 demonstrated that the optimized LPHNs (NOR-5) would be stable during storage at various temperatures [46]. In contrast to the formulations without the helping polymer and lipid, there was a slight increase observed in PDI, particle size and zeta potential values. This increase in the particle size and zeta potential might be attributed to the additional contents of the ethyl cellulose, which can impart extra negative charge and results in slight increase in the particle size as well [41].

Helper polymers and lipids were beneficial for the encapsulation of a higher NOR content. Oleic acid and ethyl cellulose potentially formed a complex which was more interactive, resulting in high EE of NOR. These results have also been endorsed by the molecular modeling study. Such arguments for high encapsulation of drug compounds in LPHNs systems have previously been reported [47,48].

FTIR studies showed that the unprocessed sample and its prepared NOR loaded LPHNs have a similar chemical structure. Thus, no interaction of NOR and excipients was proved by FTIR spectra of unprocessed NOR and processed nanoformulations. This analysis exposed that the formation of a new complex has not been observed among the formulation components, which confirms the compatibility of the NOR with the formulation components.

The SEM images indicated the development of solid spherical LPHNs. There were no observations of any aggregates of the particles. This shows that the process and experimental conditions were well controlled to engineer the lipid polymer hybrid nanoparticles with homogenous distribution, which shows that nanoparticles are amorphous in nature. The amorphous nature of nanoparticles performs a fundamental act in solubility improve-

ment which has immense pharmaceutical significance with reference to increasing oral bioavailability of poor water soluble drugs.

The execution of powder X ray diffraction was exercised for ascertaining crystallinity of the optimized formulations and compared with unprocessed NOR, lipid and helping polymer. In the LPHNs system, some of the XRD peaks for NOR materialized with tiny intensities that occurred because of particle size reduction [43]. This study demonstrated that NOR is present within the hybrid system in nanocrystalline form. In the engineered LPHNs, the consequential lipid and helping polymer peaks demonstrated the homogeneous NOR distribution within the lipid polymer hybrid system and transformation to an amorphous form. A little expansion in the width of the endothermic neither peak for NOR was noted, revealing a notable decline in particle size and conversion to amorphous form. Furthermore, a reduction in the peak intensity showing NOR and little shift towards the low melting point demonstrates a reduction in the particle size and packing density [43]. Commanding peaks of the lipid and helping polymer in the generated LPHNs directly manifest a productive entrapment of the drug molecules within the hybrid delivery system. A new peak was not engendered by the produced LPHNs. It demonstrated that the drug maintained its nature in the hybrid system and no phase transition occurred.

The previous study about the LPHNs for other drugs have also resulted in such pattern of DSC thermograms [47]. It is evident from stability studies that the planned loaded NOR-LPHNs were stable under various conditions (Figures 8 and 9). The stored samples of the prepared LPHNs were observed episodically and were found to be stable, which exhibits that the experimental and process conditions were controlled for the production of stable hybrid nanoparticles. A very insignificant growth was observed in the particle size of the samples stored at a higher temperature compared to the samples stored at refrigerator temperature. The slight increase in the solubility of the drug nanoparticles at slightly high temperature may lead to particle size growth, which has also been previously reported [40].

Among the different formulations, the LPHNs with helping polymers and lipids, which include NOR-4 and NOR-5, demonstrated a slower drug release compared to the other formulations. This reflects that NOR might be effectively encapsulated within the oleic acid and ethyl cellulose system when used as the helper lipid and polymers, respectively. The modelling studies demonstrated that the addition of the copolymer and lipid established a more rigid combined matrix structure that allowed small contents of the drug to be diffused out at regular time intervals from the polymeric and lipid shell. In our formulated lipid polymer hybrid system, the OA and ethyl cellulose further improved the retaining power of the NOR within the hybrid matrix system which was endorsed by the molecular modelling studies resulting in the highest binding energy for NOR5 (−5.9 kcal/mol) compared to the other complexes. The input of in vitro drug release data into mathematical kinetic models exposed that it best fitted into a zero-order kinetic model (i.e., drug release from LPHNs is not dependent on the amount of drug still existing in LPHNs) with R^2 values in the range of 0.935 to 0.981 for NOR (Table 5) [49]. However, in the Korsmeyer–Peppas model the value of n (the release exponent) exceeded 0.5 ($n > 0.5$) which demonstrated that the release mechanism of drugs from LPHNs has been changed from diffusion-controlled to anomalous transport (non-Fickian diffusion kinetics).

The increase in bioavailability of NOR in the form of LPHNs can be attributed to its small particle size, which in turn enhances saturation solubility, dissolution, and finally results in rapid absorption to the blood stream [50]. The liver and spleen have been reported as the two major organs for the distribution and metabolism of the solid lipid nanoparticles [51]. In addition, other studies have also reported that high doses of the SLNs caused toxicity because of accumulation of the high contents of the lipid in liver and spleen [52].

The addition of helper lipid (oleic acid) and helper polymer (ethyl cellulose) improved drug release and drug encapsulation. Integrated drug energy with lipid and polymer play a vital role in the successful encapsulation of drugs when it comes to lipid and polymer based nanoparticulate drug delivery systems. It may be inputted to high energy stearic

acid with NOR, OA, Eudragit and SLS that leads to maximum efficiency and drug loading capacity. When the link between drug and helper polymer/lipid grows, it results in excessive entrapment efficiency, in contrast to the formulations without helping polymer and surfactant [47].

The interesting results obtained from the statistical analysis of *in vivo* pharmacokinetics data confirmed that oral bioavailability was boosted with a sustained release profile for the prepared capsules of NOR compared to marketed products. The prepared capsules of NOR showed comparatively enhanced oral bioavailability, as the average particle size of the prepared nanoformulations was less than 400 nm which can easily cross the gastro-intestinal cells linings for to achieve the desired boosted oral bioavailability [53]. The relative PK analysis assisted the *in vitro* dissolution data and the polymer hybrid nanoparticles were productive due to the increased drug plasma concentration and the upgraded half-life. As compared to marketed products, the prepared capsules of NOR have particles of decreased size with increased surface area, and therefore have much more exposed surface molecules to react with the medium, which plays a vital role in enhancing the solubility as well as oral bioavailability [54]. LPHNs also have adhesive properties that could increase the residence time for drug loaded LPHNs in its administered area and hence lead to enhanced oral bioavailability [55]. Moreover, a sustained drug release profile has been exhibited by drug loaded LPHNs, which may be due to the fabricated particles being of the 100–200 nm size range, since particle sizes less than 200 nm are undetectable to the Reticulo-Endothelial System (RES) and remain in the circulatory system for a prolonged time period [56].

The obtained results for NOR loaded LPHNs clearly indicates that the hybrid system can provide the best drug delivery strategy for the formulation of potential drug candidates belonging to BCS-II and BCS-IV, to consequently boost their bioavailability with sustained release behaviour. LPHNs are not only responsible for improvement of oral absorption, but can correspondingly be formulated for parenteral administration, which needs additional studies [57].

5. Conclusions

Stable NOR loaded LPHNs were successfully produced using simple stirring and the probe sonication method. The key process and experimental conditions including concentrations of polymers and lipids, stirring rate, sonication and stirring time were optimized for stable LPHNs. The impact of helping polymers and lipids were found to be significant in EE and DLC of the NOR. The sustained release rate of the NOR from LPHNs were strongly increased by the addition of the helping polymer Ethyl cellulose, and the helper lipid oleic acid, into the developed formulations. *In vivo* pharmacokinetic studies of the engineered LPHNs showed a significant increase in drug plasma concentration and half-life elimination compared to the raw and marketed formulations. The molecular modelling studies provided molecular insight into the mechanism driving the polymer drug interaction and their impact on the drug release pattern. In future, this system can potentially be employed for the delivery of the other hydrophobic drugs.

Author Contributions: Conceptualization, M.A.K., M.S. (Muhammad Shahid), S.U.K. and M.K. (Mahwish Kmaran); conducted the experiments, simulations studies and writing—original draft, S.K., M.K. (Mohsin Kazi) and S.M.A.; supervision, M.S. (Muhammad Sohail), M.S. (Muhammad Shafique) and Z.H.; validation, H.E.T. and M.W.; reference style editing, A.E. and H.A.H.; review and editing. All authors have read and agreed to the published version of the manuscript.

Funding: The authors are thankful to the Researcher Supporting Project (number RSP-2021/146) at King Saud University, Riyadh, Saudi Arabia, and the article processing charge (APC) is also supported by RSP.

Institutional Review Board Statement: The study was conducted according to the guidelines of University of Malakand approved by Ethical committee (Notification Ref: Pharma/ECC/HA-112-4-15).

Informed Consent Statement: Not applicable.

Data Availability Statement: Not applicable.

Acknowledgments: We are thankful to King Saud University KSA and University of Malakand for providing us the financial and lab resources for concluding this project.

Conflicts of Interest: The authors declare no conflict of interest.

References

1. McArthur, D.B. Emerging infectious diseases. *Nurs. Clin. North Am.* **2019**, *54*, 297. [[CrossRef](#)] [[PubMed](#)]
2. Luepke, K.H.; Mohr, J.F. The antibiotic pipeline: Reviving research and development and speeding drugs to market. *Expert Rev. Anti-Infect. Ther.* **2017**, *15*, 425–433. [[CrossRef](#)] [[PubMed](#)]
3. Fraunfelder, F.W.; Fraunfelder, F.T. Diplopia and Fluoroquinolones. *Ophthalmology* **2009**, *116*, 1814–1817. [[CrossRef](#)]
4. Malik, O.A.A. Role of antimicrobials in the treatment of adult patients presenting to the emergency department with acute gastroenteritis - A mini review. *Pak. J. Med. Sci.* **2017**, *33*, 488–492. [[CrossRef](#)]
5. Guo, Y.; Xu, T.; Bao, C.; Liu, Z.; Fan, J.; Yang, R.; Qin, S. Design and synthesis of new norfloxacin-1,3,4-oxadiazole hybrids as antibacterial agents against methicillin-resistant *Staphylococcus aureus* (MRSA). *Eur. J. Pharm. Sci.* **2019**, *136*, 104966. [[CrossRef](#)]
6. Sood, D.; Kumar, N.; Singh, A.; Sakharkar, M.K.; Tomar, V.; Chandra, R. Antibacterial and Pharmacological Evaluation of Fluoroquinolones: A Chemoinformatics Approach. *Genom. Inform.* **2018**, *16*, 44–51. [[CrossRef](#)]
7. Marín, P.; García-Martínez, F.; Hernández, V.; Escudero, E. Pharmacokinetics of norfloxacin after intravenous, intramuscular and subcutaneous administration to rabbits. *J. Veter. Pharmacol. Ther.* **2017**, *41*, 137–141. [[CrossRef](#)]
8. Mehta, M.U.; Uppoor, R.S.; Conner, D.P.; Seo, P.; Vaidyanathan, J.; Volpe, D.A.; Stier, E.; Chilukuri, D.; Dorantes, A.; Ghosh, T.; et al. Impact of the US FDA “Biopharmaceutics Classification System” (BCS) Guidance on Global Drug Development. *Mol. Pharm.* **2017**, *14*, 4334–4338. [[CrossRef](#)] [[PubMed](#)]
9. Bhattacharya, B.; Mondal, A.; Soni, S.R.; Das, S.; Bhunia, S.; Raju, K.B.; Ghosh, A.; Reddy, C.M. Multidrug salt forms of norfloxacin with non-steroidal anti-inflammatory drugs: Solubility and membrane permeability studies. *CrystEngComm* **2018**, *20*, 6420–6429. [[CrossRef](#)]
10. Bueno, M.S.; Chierentini, L.; Bongioanni, A.; Salgado, H.R.N.; Longhi, M.R.; Garnerio, C. β -cyclodextrin complexation as an approach to enhance the biopharmaceutical properties of Norfloxacin B Hydrate. *Carbohydr. Res.* **2019**, *485*, 107818. [[CrossRef](#)] [[PubMed](#)]
11. Liu, S.; Li, M.; Jia, L.; Chen, M.; Du, S.; Gong, J. Investigation of Drug–Polymer Miscibility, Molecular Interaction, and Their Effects on the Physical Stabilities and Dissolution Behaviors of Norfloxacin Amorphous Solid Dispersions. *Cryst. Growth Des.* **2020**, *20*, 2952–2964. [[CrossRef](#)]
12. Kumar, A.; Kumar, J. Solid Dispersion Techniques: A Review. *Int. J. Res. Eng. Sci. Manag.* **2021**, *4*, 104–111.
13. Gadade, D.D.; Pekamwar, S.S. Cyclodextrin Based Nanoparticles for Drug Delivery and Theranostics. *Adv. Pharm. Bull.* **2020**, *10*, 166–183. [[CrossRef](#)] [[PubMed](#)]
14. Ndlovu, S.T.; Ullah, N.; Khan, S.; Ramharack, P.; Soliman, M.; De Matas, M.; Shahid, M.; Sohail, M.; Imran, M.; Shah, S.W.A.; et al. Domperidone nanocrystals with boosted oral bioavailability: Fabrication, evaluation and molecular insight into the polymer-domperidone nanocrystal interaction. *Drug Deliv. Transl. Res.* **2019**, *9*, 284–297. [[CrossRef](#)] [[PubMed](#)]
15. Angelova, A.; Drechsler, M.; Garamus, V.M.; Angelov, B. Pep-Lipid Cubosomes and Vesicles Compartmentalized by Micelles from Self-Assembly of Multiple Neuroprotective Building Blocks Including a Large Peptide Hormone PACAP-DHA. *ChemNanoMat* **2019**, *5*, 1381–1389. [[CrossRef](#)]
16. Angelova, A.; Drechsler, M.; Garamus, V.M.; Angelov, B. Liquid Crystalline Nanostructures as PEGylated Reservoirs of Omega-3 Polyunsaturated Fatty Acids: Structural Insights toward Delivery Formulations against Neurodegenerative Disorders. *ACS Omega* **2018**, *3*, 3235–3247. [[CrossRef](#)] [[PubMed](#)]
17. Hadinoto, K.; Sundaresan, A.; Cheow, W.S. Lipid–polymer hybrid nanoparticles as a new generation therapeutic delivery platform: A review. *Eur. J. Pharm. Biopharm.* **2013**, *85*, 427–443. [[CrossRef](#)]
18. Dave, V.; Tak, K.; Sohga, A.; Gupta, A.; Sadhu, V.; Reddy, K.R. Lipid-polymer hybrid nanoparticles: Synthesis strategies and biomedical applications. *J. Microbiol. Methods* **2019**, *160*, 130–142. [[CrossRef](#)]
19. Sonje, A.; Chandra, A. A comprehensive review on Eudragit polymer. *Int. Res. J. Pharmacy* **2013**, *4*, 71–74. [[CrossRef](#)]
20. Xie, F.-M.; Zeng, K.; Li, G.-F.; Lin, Z.-F.; Sun, L.-D. Preparation of stearic acid solid lipid nanoparticles containing podophyllotoxin. *Acad. J. First Med Coll. PLA* **2005**, *25*, 99–101.
21. Rahim, H.; Sadiq, A.; Khan, S.; Amin, F.; Ullah, R.; Shahat, A.A.; Mahmood, M.H. Fabrication and characterization of glimepiride nanosuspension by ultrasonication-assisted precipitation for improvement of oral bioavailability and in vitro α -glucosidase inhibition. *Int. J. Nanomed.* **2019**, *14*, 6287. [[CrossRef](#)] [[PubMed](#)]
22. Abdelwahed, W.; Degobert, G.; Stainmesse, S.; Fessi, H. Freeze-drying of nanoparticles: Formulation, process and storage considerations. *Adv. Drug Deliv. Rev.* **2006**, *58*, 1688–1713. [[CrossRef](#)]
23. Racault, C.; Langlais, F.; Naslain, R. Solid-state synthesis and characterization of the ternary phase Ti₃SiC₂. *J. Mater. Sci.* **1994**, *29*, 3384–3392. [[CrossRef](#)]

24. Ullah, N.; Khan, S.; Ahmed, S.; Govender, T.; Faidah, H.S.; de Matas, M.; Shahid, M.; Minhas, M.U.; Sohail, M.; Khurram, M. Dexibuprofen nanocrystals with improved therapeutic performance: Fabrication, characterization, in silico modeling, and in vivo evaluation. *Int. J. Nanomed.* **2018**, *13*, 1677–1692. [[CrossRef](#)]
25. Bhardwaj, U.; Burgess, D.J. A novel USP apparatus 4 based release testing method for dispersed systems. *Int. J. Pharm.* **2010**, *388*, 287–294. [[CrossRef](#)] [[PubMed](#)]
26. Moffat, A.C.; Osseston, M.D.; Widdop, B.; Watts, J. Clarke's Analysis of Drugs and Poisons. In *Pharmaceuticals, Body Fluids and Postmortem Materials*; Pharmaceutical Press: London, UK, 2011; Volume 12004.
27. Roohullah, Z.I.; Nasir, F.; Akhlaq, M.; Sadozai, S.K.; Zada, A.; Khan, A. Sustained release carbamezapine matrix tablets prepared by solvent-evaporation technique using different polymers. *Middle-East J. Sci. Res.* **2013**, *15*, 1368–1374.
28. Kamble, R.; Sharma, S.; Mehta, P. Norfloxacin mixed solvency based solid dispersions: An in-vitro and in-vivo investigation. *J. Taibah Univ. Sci.* **2017**, *11*, 512–522. [[CrossRef](#)]
29. OECD. OECD (Organization for Economic Co-Operation and Development) Revised Draft Guidelines 423, OECD Guidelines for the Testing of Chemicals 2001; Organization for Economic Co-operation and Development: Paris, France, 2001.
30. Krieger, E.; Vriend, G. YASARA View molecular graphics for all devices from smart phones to workstations. *Bioinformatics* **2014**, *30*, 2981–2982. [[CrossRef](#)]
31. Dallakyan, S.; Olson, A.J. Small-molecule library screening by docking with PyRx. *Methods Mol. Biol.* **2015**, *1263*, 243–250. [[CrossRef](#)]
32. Trott, O.; Olson, A.J. AutoDock Vina: Improving the speed and accuracy of docking with a new scoring function, efficient optimization, and multithreading. *J. Comput. Chem.* **2010**, *31*, 455–461. [[CrossRef](#)]
33. Pettersen, E.F.; Goddard, T.D.; Huang, C.C.; Couch, G.S.; Greenblatt, D.M.; Meng, E.C.; Ferrin, T.E. UCSF Chimera-A visualization system for exploratory research and analysis. *J. Comput. Chem.* **2004**, *25*, 1605–1612. [[CrossRef](#)]
34. Zur Mühlen, A.; Mehnert, W. Drug release and release mechanism of prednisolone loaded solid lipid nanoparticles. *Pharmazie* **1998**, *53*, 552–555.
35. Sadiq, A.A.; Abdul Rassol, A. Formulation and evaluation of silibinin loaded solid lipid nanoparticles for peroral use targeting lower part of gastrointestinal tract. *Int. J. Pharm. Pharm. Sci.* **2014**, *6*, 55–67.
36. Barzegar-Jalali, M. Kinetic Analysis of Drug Release from Nanoparticles. *J. Pharm. Pharm. Sci.* **2008**, *11*, 167–177. [[CrossRef](#)] [[PubMed](#)]
37. Zhang, Z.; Gao, F.; Bu, H.; Xiao, J.; Li, Y. Solid lipid nanoparticles loading candesartan cilexetil enhance oral bioavailability: In vitro characteristics and absorption mechanism in rats. *Nanomed. Nanotechnol. Biol. Med.* **2012**, *8*, 740–747. [[CrossRef](#)]
38. Ahmed, S.; Govender, T.; Khan, I.; Rehman, N.U.; Ali, W.; Shah, S.M.H.; Khan, S.; Hussain, Z.; Ullah, R.; Alsaid, M.S. Experimental and molecular modeling approach to optimize suitable polymers for fabrication of stable fluticasone nanoparticles with enhanced dissolution and antimicrobial activity. *Drug Des. Dev. Ther.* **2018**, *12*, 255–269. [[CrossRef](#)] [[PubMed](#)]
39. Hameed, H.A.; Khan, S.; Shahid, M.; Ullah, R.; Bari, A.; Ali, S.S.; Hussain, Z.; Sohail, M.; Khan, S.U.; Htar, T.T. Engineering of Naproxen Loaded Polymer Hybrid Enteric Microspheres for Modified Release Tablets: Development, Characterization, in silico Modelling and in vivo Evaluation. *Drug Des. Dev. Ther.* **2020**, *14*, 27–41. [[CrossRef](#)]
40. Khan, M.A.; Khan, S.; Shahid, M.; Raza, A.; Hussain, Z.; Sohali, M.; Minhas, M.U.; Shah, S.W.A.; Khan, N.; Khan, J.; et al. Clarithromycin loaded lipid polymer hybrid nanoparticles: Fabrication, in vitro and in vivo evaluation. *Pak. J. Pharm. Sci.* **2020**, *33*, 1303–1313.
41. Wu, X.; Zhang, L.; Zhang, X.; Zhu, Y.; Wu, Y.; Li, Y.; Li, B.; Liu, S.; Zhao, J.; Ma, Z. Ethyl cellulose nanodispersions as stabilizers for oil in water Pickering emulsions. *Sci. Rep.* **2017**, *7*, 12079. [[CrossRef](#)] [[PubMed](#)]
42. Matteucci, M.E.; Hotze, M.A.; Johnston, K.P.; Williams, R.O. Drug Nanoparticles by Antisolvent Precipitation: Mixing Energy versus Surfactant Stabilization. *Langmuir* **2006**, *22*, 8951–8959. [[CrossRef](#)]
43. Khan, S.; De Matas, M.; Zhang, J.; Anwar, J. Nanocrystal Preparation: Low-Energy Precipitation Method Revisited. *Cryst. Growth Des.* **2013**, *13*, 2766–2777. [[CrossRef](#)]
44. Li, D.; Kaner, R.B. Shape and Aggregation Control of Nanoparticles: Not Shaken, Not Stirred. *J. Am. Chem. Soc.* **2006**, *128*, 968–975. [[CrossRef](#)] [[PubMed](#)]
45. Dora, C.P.; Singh, S.K.; Kumar, S.; Datusalia, A.K.; Deep, A. Development and characterization of nanoparticles of glibenclamide by solvent displacement method. *Acta Pol. Pharm. Drug Res.* **2010**, *67*, 283–290.
46. Lestari, M.L.A.D.; Müller, R.H.; Möschwitzer, J.P. Systematic Screening of Different Surface Modifiers for the Production of Physically Stable Nanosuspensions. *J. Pharm. Sci.* **2015**, *104*, 1128–1140. [[CrossRef](#)]
47. Seedat, N.; Kalhapure, R.; Mocktar, C.; Vepuri, S.; Jadhav, M.; Soliman, M.; Govender, T. Co-encapsulation of multi-lipids and polymers enhances the performance of vancomycin in lipid-polymer hybrid nanoparticles: In vitro and in silico studies. *Mater. Sci. Eng. C* **2016**, *61*, 616–630. [[CrossRef](#)]
48. Sonawane, S.J.; Kalhapure, R.S.; Rambharose, S.; Mocktar, C.; Vepuri, S.B.; Soliman, M.; Govender, T. Ultra-small lipid-dendrimer hybrid nanoparticles as a promising strategy for antibiotic delivery: In vitro and in silico studies. *Int. J. Pharm.* **2016**, *504*, 1–10. [[CrossRef](#)]
49. Costa, P.; Sousa Lobo, J.M. Modeling and comparison of dissolution profiles. *Eur. J. Pharm. Sci.* **2001**, *13*, 123–133. [[CrossRef](#)]
50. Al-Thamarani, S.; Gardouh, A. Enhanced oral bioavailability and gastroprotective effect of ibuprofen through mixed polymer-lipid nanoparticles. *Ther. Deliv.* **2021**, *12*, 363–374. [[CrossRef](#)]

51. Blasi, P.; Giovagnoli, S.; Schoubben, A.; Ricci, M.; Rossi, C. Solid lipid nanoparticles for targeted brain drug delivery. *Adv. Drug Deliv. Rev.* **2007**, *59*, 454–477. [[CrossRef](#)]
52. Weyhers, H.; Ehlers, S.; Hahn, H.; Souto, E.B.; Müller, R.H. Solid lipid nanoparticles (SLN)–Effects of lipid composition on in vitro degradation and in vivo toxicity. *Die Pharm.* **2006**, *61*, 539–544.
53. Suh, W.H.; Suslick, K.; Stucky, G.D.; Suh, Y.-H. Nanotechnology, nanotoxicology, and neuroscience. *Prog. Neurobiol.* **2009**, *87*, 133–170. [[CrossRef](#)]
54. Dang, L.; Yang, H.; Black, S.; Wei, H. The Effect of Temperature and Solvent Composition on Transformation of β - to α -Glycine as Monitored in Situ by FBRM and PVM. *Org. Process. Res. Dev.* **2009**, *13*, 1301–1306. [[CrossRef](#)]
55. Abbaspour, M.; Makhmalzadeh, B.; Arastoo, Z.; Jahangiri, A.; Shiralipour, R. Effect of Anionic Polymers on Drug Loading and Release from Clindamycin Phosphate Solid Lipid Nanoparticles. *Trop. J. Pharm. Res.* **2013**, *12*, 477–482. [[CrossRef](#)]
56. Bhandari, R.; Kaur, I.P. Pharmacokinetics, tissue distribution and relative bioavailability of isoniazid-solid lipid nanoparticles. *Int. J. Pharm.* **2013**, *441*, 202–212. [[CrossRef](#)]
57. Yang, S.C.; Lu, L.F.; Cai, Y.; Zhu, J.B.; Liang, B.W.; Yang, C.Z. Body distribution in mice of intravenously injected camptothecin solid lipid nanoparticles and targeting effect on brain. *J. Control. Release* **1999**, *59*, 299–307. [[CrossRef](#)]